

# Dynamical quantum phase transition of a two-component Bose-Einstein condensate in an optical lattice

Anssi Collin, Jani-Petri Martikainen, and Jonas Larson\*

*NORDITA, 106 91 Stockholm, Sweden*

(Dated: November 19, 2018)

We study dynamics of a two-component Bose-Einstein condensate where the two components are coupled via an optical lattice. In particular, we focus on the dynamics as one drives the system through a critical point of a first order phase transition characterized by a jump in the internal populations. Solving the time-dependent Gross-Pitaevskii equation, we analyze; breakdown of adiabaticity, impact of non-linear atom-atom scattering, and the role of a harmonic trapping potential. Our findings demonstrate that the phase transition is resilient to both contact interaction between atoms and external trapping confinement.

PACS numbers: 03.75.Mn,64.60.Ht,64.70.Tg,67.85.Hj

## I. INTRODUCTION

Since the pioneering experiments on Bose-Einstein condensates (BEC) [1], the field of ultracold atomic gases has seen a tremendous development [2]. Nowadays, preparation and manipulation of BECs is a standard procedure providing a versatile testbed for the study of various quantum effects. Spinor condensates, where internal atomic Zeeman levels play an important role for the dynamics, have been experimentally studied by numerous groups [3]. More recent experiments on spinor condensates include; coherent transport [4], spin-mixing [5], inherent spin tunneling [6], and symmetry breaking [7]. Placing the condensate in an optical lattice formed by counter propagating laser beams greatly affects its characteristics and exciting phenomena, *e.g.* Bloch oscillations [8], gap and colliding solitons [9, 10], self-trapping [11], superfluid instability [12], vortices [13], Anderson localization [14], and for more strongly correlated systems the superfluid-Mott insulator phase transition (PT) [15], arise.

Most theoretical works studying PTs consider systems at strict thermal equilibrium. However, a more appropriate picture capturing the underlying physics of real experiments is often encountered by a dynamical approach. Indeed, the great experimental progress seen in the recent past on correlated ultracold atomic systems [16], calls for a deeper theoretical understanding of non-equilibrium PTs. Much of the theoretical works are devoted to dynamics across a critical point in various spin models [17, 18, 19, 20, 21]. Also the dynamics of phase transitions in lattice many-body systems such as the Bose-Hubbard model have been considered [22, 23]. To derive an estimate of the adiabatic breakdown, the Landau-Zener formula, giving a measure of transition probabilities across an avoided level crossing [24], has been utilized in most of the above works [17, 18, 19, 20, 22]. Moreover,

in Refs. [17, 18, 19, 22, 23] the Kibble-Zurek mechanism of quench induced transitions was employed.

In this paper we consider a spinor condensate in an optical lattice. Apart from providing an effective periodic potential, in this model the lattice also induces a coupling between the internal atomic states. The corresponding many-body model, without atom-atom interactions, was first introduced in Ref. [25], and the occurrence of a first order PT between different internal states was demonstrated. The system was further investigated in [26] by taking interaction between the atoms into account. Both of these works consider thermodynamical equilibrium. Since the single particle ground state of the present model is not gapped, even small time-dependent perturbations of the Hamiltonian might well cause non-adiabatic excitations. Driven through the critical point, such excitations might wash out the signatures of the PT. One goal of the present paper is to study the importance of these non-adiabatic contributions. Moreover, the model automatically takes into account the effects deriving from atom-atom interactions, and the state changing collisions they bring about. This aspect was left as an open question in [25]. In addition, the sensitivity to external harmonic trapping is also considered.

The outline of the paper is as follows. In the next section, we present the one dimensional single particle Hamiltonian. After first discussing some general properties in Subsec. II A, we numerically diagonalize the Hamiltonian and give the spectrum in Subsec. II B. Using the spectrum, we demonstrate the equilibrium PT in Subsec. II C. The following Sec. III is devoted to our main results; the dynamics when the system is driven through the critical point. The numerical method for solving the Gross-Pitaevskii equations is outlined, and first the thermal equilibrium PT is studied by means of the partial-state fidelity susceptibility. In Subsec. III A we calculate the order parameter for different dimensions, whereby the following Subsection considers the situation of external harmonic trapping. Breakdown of adiabaticity is analyzed in Subsec. III C. Finally we conclude in Sec. IV.

---

\*Electronic address: jolarson@kth.se

## II. ONE DIMENSIONAL IDEAL GAS MODEL SYSTEM

The appearance and nature of the PT are easily extracted from the structure of the spectrum of the one dimensional single particle Hamiltonian. The effects of particle interactions, higher dimensional systems, and explicit time-dependence of system parameters will be considered in Sec. III.

### A. Ideal gas Hamiltonian

The properties of an ideal gas are captured in the corresponding single particle system. We consider a three-level  $\Lambda$  atom dipole coupled to two light fields as illustrated in Fig. 1. The  $1 \leftrightarrow 3$  transition is driven via a periodic standing wave field, while an “external” spatially independent laser gives rise to the  $2 \leftrightarrow 3$  transition. This assumes the perpendicular laser to have a mode-waist larger than the extent of the condensate. The effective atom-field couplings are  $\lambda$  and  $\Omega$ , the wave number  $k$ , and the atom-field detunings  $\delta_1$  and  $\delta_2$  respectively. In the case of large detunings, the excited atomic state  $|3\rangle$  may be adiabatically eliminated yielding an effective  $2 \times 2$  Hamiltonian [27]

$$\hat{H}_1 = \frac{\hat{p}^2}{2m} + \frac{\hbar\tilde{\Delta}}{2}\hat{\sigma}_z - \hbar\tilde{U}_1 \cos(2k\hat{x})\hat{\sigma}_{11} + \hbar\tilde{U} \cos(k\hat{x})\hat{\sigma}_x, \quad (1)$$

where  $\tilde{\Delta} = |\delta_1 - \delta_2| - \Omega^2/\delta_2 - \lambda^2/2\delta_1$  is an effective detuning taking into account for the constant Stark shifts of states 1 and 2,  $\tilde{U}_1 = \lambda^2/2\delta_1$ ,  $\tilde{U} = \lambda\Omega(1/2\delta_1 + 1/2\delta_2)$ , and the  $\sigma$ -operators are the Pauli matrices;  $\hat{\sigma}_z = |2\rangle\langle 2| - |1\rangle\langle 1|$ ,  $\hat{\sigma}_x = |1\rangle\langle 2| + |2\rangle\langle 1|$ , and  $\hat{\sigma}_{11} = |1\rangle\langle 1|$ . Respectively,  $\hat{p}$ ,  $\hat{x}$ , and  $m$  are atomic momentum, position and mass. Note that the  $\tilde{U}_1$  term originates from the Stark shift of the  $|1\rangle$  state. As it affects only the  $|1\rangle$  state and not the  $|2\rangle$  state, it shifts the detuning resonance  $\tilde{\Delta}_c = 0 \rightarrow \tilde{\Delta}_c \neq 0$ . Apart from altering the detuning resonance, it also renders a light induced potential for the state  $|1\rangle$ . The  $\tilde{U}$  term, on the other hand, provides an effective potential for both internal states. In the limiting cases, when one of the parameters  $\tilde{\Delta}$ ,  $\tilde{U}_1$  and  $\tilde{U}$  is dominating the other two, it is legitimate to assign a particular potential to the internal atomic states. In general, however, the full coupled system has to be considered as an entity [26].

For later convenience, scaled quantities are introduced by the characteristic energy and length scales  $E_r = \frac{\hbar^2 k^2}{2m}$  and  $k^{-1}$ , such that

$$\hat{x} = k\hat{\tilde{x}}, \quad \Delta = \frac{\hbar\tilde{\Delta}}{E_r}, \quad U_1 = \frac{\hbar\tilde{U}_1}{E_r}, \quad U = \frac{\hbar\tilde{U}}{E_r}. \quad (2)$$

In the matrix-form, the scaled Hamiltonian reads

$$\hat{H}_1 = -\frac{\partial^2}{\partial x^2} + \begin{bmatrix} \frac{\Delta}{2} & U \cos(\hat{x}) \\ U \cos(\hat{x}) & -\frac{\Delta}{2} - U_1 \cos(2\hat{x}) \end{bmatrix}, \quad (3)$$

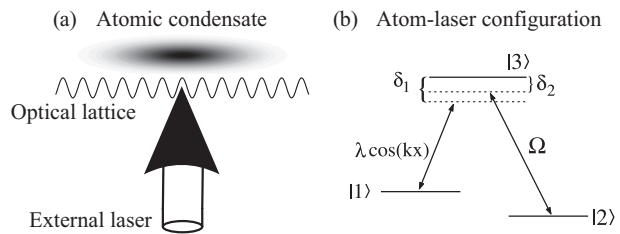


FIG. 1: Schematic configuration of system setup (a) and atom-laser configuration (b). An optical lattice drives the  $|1\rangle \leftrightarrow |3\rangle$  atomic transition and the “external” laser the  $|2\rangle \leftrightarrow |3\rangle$  transition.

where we have  $|1\rangle = \begin{bmatrix} 0 \\ 1 \end{bmatrix}$  and  $|2\rangle = \begin{bmatrix} 1 \\ 0 \end{bmatrix}$ . From the fact that  $\cos(\hat{x})|q\rangle = (|q+1\rangle + |q-1\rangle)/2$ , where  $\hat{p}|q\rangle = q|q\rangle$ , one finds that a swapping of the internal states 1 and 2 is accompanied by a shift of momentum by one unit in either positive or negative direction. Moreover, a given momentum eigenstate  $|q\rangle$  is only coupled to other momentum states  $|q+\eta\rangle$ , where  $\eta$  is any integer. In particular, the states  $\{|q\rangle|i\rangle\}$  ( $i = 1, 2$ ) can be divided into two sets

$$|\varphi_\eta(q)\rangle = \begin{cases} |q+\eta\rangle|2\rangle & \eta \text{ even} \\ |q+\eta\rangle|1\rangle & \eta \text{ odd} \end{cases} \quad (4)$$

$$|\phi_\eta(q)\rangle = \begin{cases} |q+\eta\rangle|1\rangle & \eta \text{ even} \\ |q+\eta\rangle|2\rangle & \eta \text{ odd}, \end{cases}$$

which are not coupled by the Hamiltonian (3);  $\langle\varphi_{\eta'}(q')|\hat{H}_1|\phi_\eta(q)\rangle = 0$ . Thus, the Hamiltonian may be written as  $\hat{H}_1 = \hat{H}_\varphi \otimes \hat{H}_\phi$ , where the two sub-Hamiltonians operate on states spanned by  $\{|\varphi_\eta(q)\rangle\}$  or  $\{|\phi_\eta(q)\rangle\}$  respectively. Here, the quasi momentum  $q$  resides in the first Brillouin zone.

As a periodic operator,  $\hat{H}_1$  commutes with  $\hat{T} = e^{\pm il\hat{p}}$ , where  $l = 2\pi$  is the scaled period. It is readily shown [28] that the operator

$$\hat{I} = \hat{\sigma}_z e^{\pm i\frac{l}{2}\hat{p}}, \quad (5)$$

defines another symmetry, describing a half-period boost of the position and an atomic inversion. An outcome of this  $l/2$  symmetry is that the Brillouin zone extends beyond  $(-\pi/l, \pi/l]$  as imposed by the  $l$ -periodicity of the system [25, 28]. Thereby, the first Brillouin zone is instead defined for quasi momentum  $q \in (-1, 1]$ .

### B. Ideal gas energy spectrum

As was already pointed out, the character of the PT is directly seen from the energy spectrum. Due to the block diagonal form of the Hamiltonian,  $\hat{H}_1 = \hat{H}_\varphi \otimes \hat{H}_\phi$ , the dispersions of  $\hat{H}_\varphi$  and  $\hat{H}_\phi$  can be calculated separately.

In the figures, we will differentiate between dispersions of  $\hat{H}_\varphi$  and  $\hat{H}_\phi$  by using dashed or solid curves, respectively.

The internal two-level structure of the system brings about anomalous dispersions that possess several minima [26, 29]. The lowest energy of each band  $E_\nu(q)$ , where  $\nu = 1, 2, 3, \dots$  is the band index and  $q \in (-1, 1]$  the quasi momentum, is twofold degenerate. However, the degeneracy is due to the fact that the individual energy bands  $E_\nu^{(\varphi)}(q) = E_\nu^{(\phi)}(q')$  for some  $q$  and  $q'$ . The only exception is at exact resonance  $\Delta = \Delta_c$ , where the bands  $E_\nu^{(\varphi)}(q)$  and  $E_\nu^{(\phi)}(q)$  become identical.

The Hamiltonian (3) is readily diagonalized by truncating the number of basis states (4). If  $U_1 \gg U$ , atoms in the  $|1\rangle$  state will feel a strong periodic potential, while  $|2\rangle$  atoms experience only a weak potential. Thus, the spectrum is in this case typically made up of a fairly flat band mixed together with “parabolic” energy bands. When  $U$  dominates  $U_1$ , the situation is different and mixing of flat and “parabolic” bands does not exist. Examples of the first three energy dispersions are displayed in Fig. 2. In (a)-(d)  $U > U_1$ , while in (e)-(h)  $U_1 \gg U$ . In the last three plots, almost flat dispersions are found due to the large  $U_1$ , and especially in (f) there are “parabolic” bands with lower energy than the flat one.

### C. First order phase transition

At zero temperature, the condensate atoms will occupy the ground state. Even though the ground state is degenerate, mainly one of the degenerate states will be populated. In an experiment, the atoms will typically be initialized in either  $|1\rangle$  or  $|2\rangle$  and then cooled down to its ground state. Hence, the obtained initial ground state will predominantly populate either of the two energy bands  $E_1^{(\varphi)}(q)$  or  $E_1^{(\phi)}(q)$ . An equal population balance between the degenerate ground states is very unlikely, and indeed, in our numerical simulations of interacting systems utilizing the imaginary time propagation method we never encounter such balanced situations.

Comparing Fig. 2 (a) and (d), it is seen that the dispersions  $E_\nu^{(\varphi)}(q)$  and  $E_\nu^{(\phi)}(q)$  have been roughly swapped when  $\Delta \leftrightarrow -\Delta$ . Thus, the minimum of  $E_1^{(\varphi)}(q)$  or  $E_1^{(\phi)}(q)$  are changed between the center and edges of the Brillouin zone as  $\Delta$  is tuned through the resonance  $\Delta = \Delta_c$ . In the example of Fig. 2 (a)-(d), this resonance condition is  $\Delta_c \approx 0$  since  $U_1 \ll 1$ . When  $U_1$  is large, however, the  $\Delta_c$  is shifted away from zero, but nonetheless, between  $\Delta < \Delta_c$  and  $\Delta > \Delta_c$  the minima is either at the Brillouin center or at its edges. As the quasi momentum corresponding to the energy minima of either  $E_1^{(\varphi)}(q)$  or  $E_1^{(\phi)}(q)$  changes abruptly when  $\Delta$  is tuned across the resonance, one encounters a first order PT.

As discussed in the previous subsection, the internal ( $|1\rangle$  and  $|2\rangle$ ) and external (momentum) degrees of freedom cannot be changed independently via the Hamil-

tonian (3). Absorption or emittance of a lattice photon always induces a momentum “kick”. Consequently, shifting the momentum of the ground state between the center and the edges of the Brillouin zone is only possible by swapping the internal states  $|1\rangle$  and  $|2\rangle$ . Thus, the collective inversion for atoms belonging to either of the  $E_1^{(\varphi)}(q)$  or  $E_1^{(\phi)}(q)$  bands

$$j_z^{(\gamma)} = \frac{1}{N_\gamma} \sum_{i=1}^{N_\gamma} \langle \hat{\sigma}_z^{(i)} \rangle, \quad \gamma = \varphi, \phi, \quad (6)$$

where  $\hat{\sigma}_z^{(i)}$  is the  $i$ th atom’s  $z$  Pauli matrix, should be discontinuous at  $\Delta_c$ . Here,  $N_\alpha$  is the number of condensate atoms in band  $E_1^{(\gamma)}(q)$ , and we note that since we consider only the ground state,  $\langle \hat{\sigma}_z^{(i)} \rangle = \langle \hat{\sigma}_z^{(j)} \rangle$  for any  $i$  and  $j$ . The full inversion  $j_z = j_z^{(\varphi)} + j_z^{(\phi)}$ , however, depends on the number of atoms residing in each band.

Figure 3 displays two examples of  $j_z$  when all atoms belong to the  $E_1^{(\phi)}(q)$  band. In (a), the inversion is shown for the parameters corresponding to Figs. 2 (a)-(d), and the gap of the inversion is found to be well resolved. In (b), however, corresponding to Figs. 2 (e)-(h), reveals a small gap in the inversion. In this case, the PT occurs for a detuning  $\Delta_c \approx 3.8$  which is somewhere between Fig. 2 (g) and (h) where the dispersions are fairly flat. We note that apart from shifting the critical resonance  $\Delta_c$ , large  $U_1$ ’s also results in asymmetric  $j_z^{(\phi)}$ ’s with respect to  $\Delta_c$ .

## III. DYNAMICAL PHASE TRANSITION OF A WEAKLY INTERACTING BOSE-EINSTEIN CONDENSATE

Section II demonstrated that a first order PT is encountered by driving the system of non-interacting atoms through a critical detuning  $\Delta_c$ . Adding interaction between the atoms will introduce coupling between the two sets of basis states (4). This effect is, however, relatively small [26]. On the other hand, very strong atom-atom scattering amplitudes can have other important consequences, for example it may drastically change the single particle dispersion curves [30]. Nonetheless, it was argued in Refs. [25, 26], that the PT should be stable even against strong interaction between the particles. In this section we will show, on a mean-field basis, that this is indeed true, and that the PT is also insensitive to an external harmonic trapping potential. Moreover, the dynamics of the condensate driven through the critical point will be thoroughly addressed.

### A. Sweep through the critical point

The spectra  $E_1^{(\varphi)}(q = 0, \Delta)$  and  $E_1^{(\varphi)}(q = \pm 1, \Delta)$ , and the spectra  $E_1^{(\phi)}(q = 0, \Delta)$  and  $E_1^{(\phi)}(q = \pm 1, \Delta)$  become

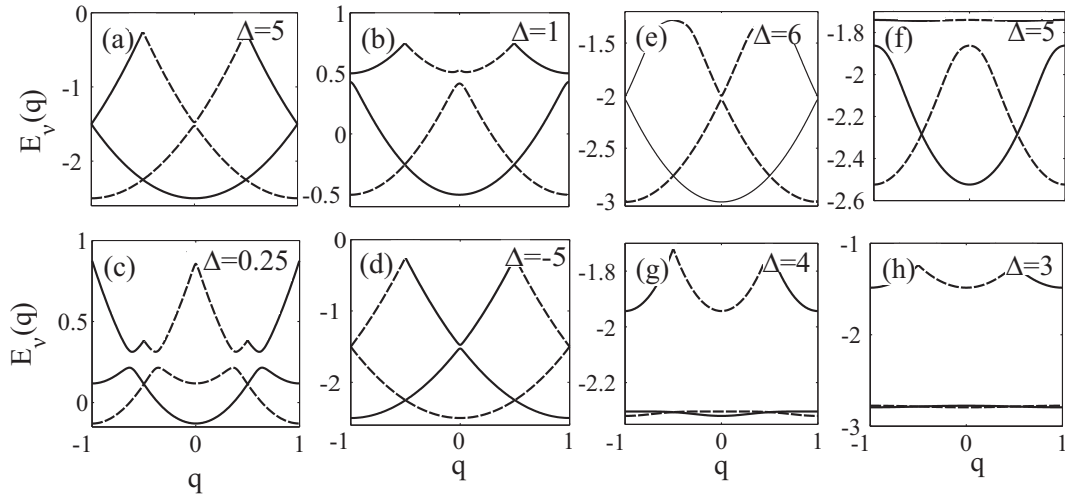


FIG. 2: Examples of the three lowest energy bands of Hamiltonian (3). In (a)-(d) we have  $U > U_1$  ( $U = 0.1$  and  $U_1 = 0.05$ ), while in (e)-(h)  $U < U_1$  ( $U = 0.2$  and  $U_1 = 8$ ). The multiple number of local minima of the lowest band is clear. Dashed lines are the energy dispersions  $E_\nu^{(\phi)}(q)$  of the sub-Hamiltonian  $\hat{H}_\phi$ , and solid lines are  $E_\nu^{(\phi)}(q)$  corresponding to  $\hat{H}_\phi$ .

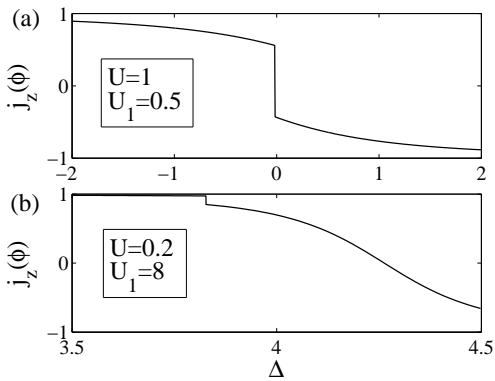


FIG. 3: The inversion (6) as function of detuning  $\Delta$ . In the upper plot,  $U_1 \ll 1$  and  $\Delta_c \approx 0$ , while in the lower plot  $U_1 = 8$  giving  $\Delta_c \approx 3.8$ .

degenerate and cross at  $\Delta = \Delta_c$ . Such crossing of energies is characteristic for a PT [31]. The crossing of energies in the present model is envisaged in Fig. 4 displaying the energies  $E_1^{(\phi)}(q, \Delta)$  as function of  $\Delta$  for  $q = -n/N$ , where  $N = 10$  and  $n = 0, 1, \dots, N$ . Letting  $N \rightarrow \infty$ , the spacings between the lines in Fig. 3 vanish. The two figures use the same parameters as in Fig. 3, and we note that when  $U_1$  is large,  $\Delta_c$  is shifted away from zero as was already seen in Fig. 3. Further, in (a) corresponding to Fig. 3 (a) where the discontinuity of the order parameter is more pronounced, the energies are more sparsely spaced compared to (b). Indeed, in (b) it is not even clear that the energies  $E_1^{(\phi)}(q = 0, \Delta)$  and  $E_1^{(\phi)}(q = \pm 1, \Delta)$  actually cross. However, a closer look around the critical point reveals the crossing.

The purpose of this section is to study the effects on

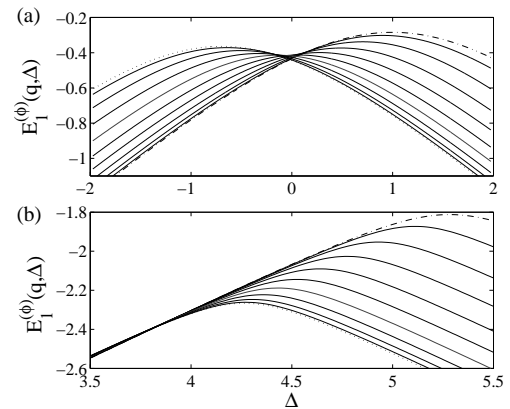


FIG. 4: Examples of the lowest band energies  $E_1^{(\phi)}(q_n, \Delta)$  for  $q_n = -n/10$ ,  $n = 0, 1, \dots, 10$ . The parameters are the same as in Fig. 3;  $U = 1$  and  $U_1 = 0.5$  in (a), and  $U = 0.2$  and  $U_1 = 8$  in (b). The dotted line and the dot-dashed line are the energies  $E_1^{(\phi)}(-1, \Delta)$  and  $E_1^{(\phi)}(0, \Delta)$  respectively, and the crossing between these two,  $E_1^{(\phi)}(0, \Delta) = E_1^{(\phi)}(-1, \Delta)$ , gives the critical detuning  $\Delta_c$ .

the PT arising from interaction between the particles and from a confining harmonic trap. Furthermore, the analysis will not be restricted to the one dimensional case, but we also considers the two dimensional counterparts. One interesting aspect is the dynamics in itself as the system is driven through the critical point. Another central aspect that will be investigated is breakdown of adiabaticity. Due to the continuous spectrum and the crossing of the energy levels, non-adiabatic excitations of the condensate are expected and especially around  $\Delta = \Delta_c$  where the density of states drastically increases.

In the higher dimensional cases we assume, for simplic-

ity, that all lattice fields couple with the same strength to the atom and that they share the same periodicity. Such a scheme requires multiple excited Zeeman levels as well as mutually orthogonal polarizations of the lattice beams, but after the adiabatic elimination on all of them, one is left with an effective two-level Hamiltonian

$$\hat{H} = -\hat{\nabla}^2 + \begin{bmatrix} \frac{\Delta}{2} & U \sum_{\alpha} \cos(x_{\alpha}) \\ U \sum_{\alpha} \cos(x_{\alpha}) & -\frac{\Delta}{2} - U_1 \sum_{\alpha} \cos^2(x_{\alpha}) \end{bmatrix}. \quad (7)$$

Here  $\alpha$  indicates a component of the vector along the direction  $\alpha$ .

Moreover, we will take into account for collisions between the particles in terms of a non-linear term in the Hamiltonian, as well as consider a harmonic trapping potential. We thus consider the Gross-Pitaevskii equation

$$\begin{aligned} i \frac{\partial}{\partial t} \Psi(\mathbf{x}, t) &= \hat{H}_{GP} \Psi(\mathbf{x}, t) \\ &= \left[ \hat{H} + \frac{\omega^2}{2} \sum_{\alpha} x_{\alpha}^2 + \Psi^{\dagger}(\mathbf{x}) \cdot \mathbf{g} \cdot \Psi(\mathbf{x}) \right] \Psi(\mathbf{x}, t), \end{aligned} \quad (8)$$

where  $t$  is the scaled time,  $\omega$  the scaled parameter determining the trap frequency, and  $\mathbf{g}$  the scattering amplitudes. In this coupled two-level problem, the wave functions are spinors

$$\Psi(\mathbf{x}) = \begin{bmatrix} \psi_2(\mathbf{x}) \\ \psi_1(\mathbf{x}) \end{bmatrix} \quad (9)$$

and

$$\mathbf{g} = \begin{bmatrix} g_{11} & g_{12} \\ g_{12} & g_{22} \end{bmatrix}. \quad (10)$$

Normalizing the wave function as  $\int d\mathbf{x} |\Psi(\mathbf{x})|^2 = 1$ , the scattering amplitudes become  $g_{ij} = 4\pi\hbar N a_{ij} / mV E_r$ , where  $N$  is the number of condensate atoms,  $V$  the effective volume, and  $a_{ij}$  the state dependent  $s$ -wave scattering amplitude.

We will solve Eq. (8) numerically, starting in the ground state for large detuning and then change  $\Delta$  in time such that it passes the critical point. In particular we chose a linear sweep of the detuning,

$$\Delta(t) = \Delta_0 t, \quad (11)$$

where  $\Delta_0$  sets the sweep velocity. We integrate (8) from large negative to large positive times  $t \in [-T, T]$  such that the critical point is surely traversed.

The GP equation (8) is solved using the split operator wave packet method [32]. The initial state is taken as the ground state for the given system parameters. In particular, the ground state is obtained via the imaginary time evolution

$$\Psi_{GS}(\mathbf{x}) = \lim_{\tau \rightarrow \infty} \frac{\Psi_{\mathbf{0}}(\mathbf{x}, \tau)}{\sqrt{\int d\mathbf{x} |\Psi_{\mathbf{0}}(\mathbf{x}, \tau)|^2}}, \quad (12)$$

where

$$\Psi_{\mathbf{0}}(\mathbf{x}, \tau) = e^{-\tau \hat{H}_{GP}} \Psi_{\mathbf{0}}(\mathbf{x}, 0) \begin{bmatrix} 1 \\ 0 \end{bmatrix} \quad (13)$$

and  $\Psi_{\mathbf{0}}(\mathbf{x}, 0)$  is the initial wave function ansatz which will be taken as a normalized real Gaussian. The subscript  $\mathbf{0}$  indicates the initial Hamiltonian parameters  $U$ ,  $U_1$ ,  $\mathbf{g}$ ,  $\Delta_0$ , and  $T$ , as well as the center of the Gaussian  $\mathbf{x}_0 = 0$  and its width  $\Delta_{\mathbf{x}}$  (which is taken to be much larger than the period  $l = 2\pi$  of the Hamiltonian). This numerical procedure gives a good approximation for the ground state. Another important point is that since the ground state (for a non-interacting system) is degenerate, the imaginary time evolution renders different states depending on the ansatz (13). In particular, since for the state of our assumption all population resides in the  $|1\rangle$  state and the momentum is centered around the origin, the ground state obtained from (12) will mainly populate states spanned by  $\{|\varphi_{\eta}(q)\rangle\}$ . This holds even for relatively large  $\mathbf{g}$ . Again, an imbalanced initial state is believed to be in good agreement with true experimental realizations; roughly speaking, the imaginary time evolution represents the cooling of the condensate.

Before studying the actual dynamic problem, we consider the PT characterized by the ground states numerically obtained via imaginary time evolution (12). By doing so, we get an idea of how sensitive the PT is to the non-linear atom-atom interaction term. In particular, we evaluate the partial-state fidelity susceptibility, which has been demonstrated to give a clear indication of various PTs [33]. The advantage of utilizing a fidelity measure, originating from the quantum information concepts, to analyzing PTs is that it is state independent and no prior knowledge about order parameters is required. The fidelity susceptibility has been shown to contain sufficient information to reveal the universality class of the PTs [34], even for topological PTs [35], Kosterlitz-Thouless transitions [34], and PTs characterized by an underlying continuous level crossing [36]. The idea is simple, letting the ground state be parameterized by some quantity  $h$  (in our case  $h = \Delta$ ),  $\rho(h) = |\Psi(h)\rangle\langle\Psi(h)|$  we introduce the reduced density operator for the internal states  $\rho_A(h) = \text{Tr}_B[\rho(h)]$ , where the trace is over external degrees of freedom. For the present model, it is straightforward to derive

$$\rho_A(h) = \begin{bmatrix} N_{11}(h) & N_{12}(h) \\ N_{21}(h) & N_{22}(h) \end{bmatrix}, \quad (14)$$

where  $N_{ij} = \int d\mathbf{x} \psi_i^*(\mathbf{x}, h) \psi_j(\mathbf{x}, h)$  and  $\psi_i(\mathbf{x}, h)$  is the constituent ground state wave function for the parameter  $h$ . The partial-state fidelity is defined as

$$F_A(h, \delta h) = \text{Tr} \left[ \sqrt{\sqrt{\rho_A(h)} \rho_A(h + \delta h) \sqrt{\rho_A(h)}} \right]. \quad (15)$$

In terms of  $F_A(h, \delta h)$ , the partial-state fidelity susceptibility reads

$$\chi(h) = \lim_{\delta h \rightarrow 0} \frac{-2 \ln F_A(h, \delta h)}{\delta h^2}. \quad (16)$$

For the situation at hand, there is a critical  $h_c (= \Delta_c)$  for which the PT occurs. The fidelity measures the overlap between the groundstates for different parameters  $h$  and  $h + \delta h$ , and whenever  $h_c$  lies between these two values the fidelity will drastically drop and the susceptibility increase. This is displayed in Fig. 5. The upper plot (a) represent the case with  $U > U_1$ , while (b) shows examples of the reverse situation. For solid lines, the atom-atom interaction is zero and for dashed lines it is non-zero. The sharp peaks of the susceptibility at  $h_c$  coincide well with the critical parameters found in Fig. 3 using the full numerical diagonalization of the single particle Hamiltonian. The slight discrepancy is believed to derive from the fact that the imaginary time propagation is stopped after some finite time  $\tau$ . Interestingly, the shape and location of the peaks of  $\chi(h)$  seems to be insensitive for atom-atom interactions, proving that the PT is not restricted to an ideal gas.

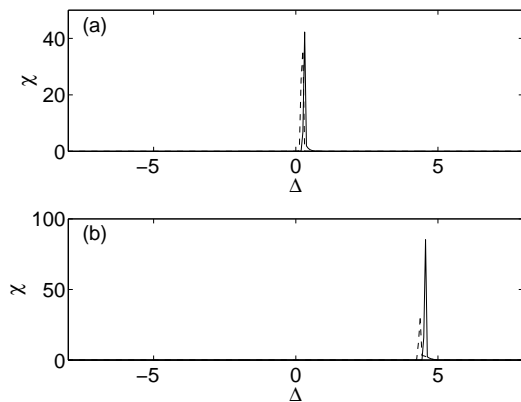


FIG. 5: The partial-state fidelity susceptibility (16) for the one dimensional model. In (a)  $U = 1$  and  $U_1 = 0.5$ , while in (b)  $U = 0.2$  and  $U_1 = 8$ . In both plots  $\omega = 0$ , and  $g_{11} = g_{22} = g_{12} = 0$  (solid lines),  $g_{11} = g_{22} = 10g_{12} = 10$  (dashed lines).

Let us now turn to dynamics. Once the ground state is initialized, the wave packet is let to evolve using the real time propagator. Since the Hamiltonian is explicitly time-dependent, the evolution is non-trivial. Figure 6 shows examples of the collective inversion  $j_z = j_z^{(\phi)} + j_z^{(\varphi)}$ , corresponding to the parameters of Fig. 3. Solid lines give the one dimensional case and dashed lines the two dimensional case. The figure makes clear that the PT is resilient to the dimensionality of the system. In fact, the change in the inversion is even more pronounced in the two dimensional situation. The shift of the critical point between the two dimensions seen in (b) can be understood from the Hamiltonian (7). Since in two dimensions the sum on the diagonal contains two terms and both terms shift the resonance condition, the shifting is larger for higher dimensions.

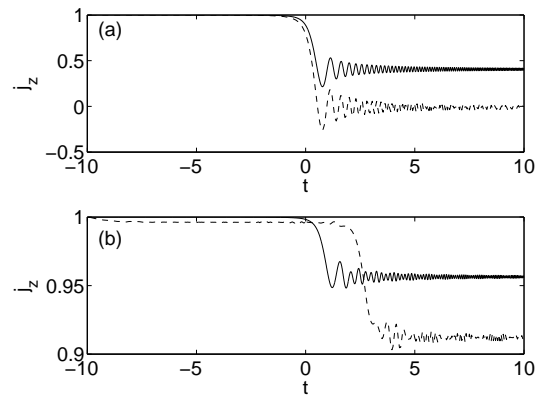


FIG. 6: Examples of the collective inversion  $j_z$  as function of time; one dimension (solid lines) and two dimensions (dashed lines). In (a)  $U = 1$  and  $U_1 = 0.5$ , while in (b)  $U = 0.2$  and  $U_1 = 8$ . In both plots  $\Delta_0 = 10$ ,  $\omega = 0$ ,  $g_{11} = g_{22} = g_{12} = 0$ .

## B. Effect of a trapping potential

The PT demonstrated in the previous section is an outcome of the periodicity of our system and in particular the anomalous energy dispersions. The band structure of the spectrum will be lost if the condensate is placed in an additional external trapping potential. For weak confinement, however, the spectrum still shows similarities to a band-gap spectrum. More precisely, if the characteristic length scale of the harmonic trap is much larger than the lattice periodicity  $l = 2\pi$ , signatures of the PT are supposedly still present. On the other hand, very tight trapping may wash out any signatures of the PT.

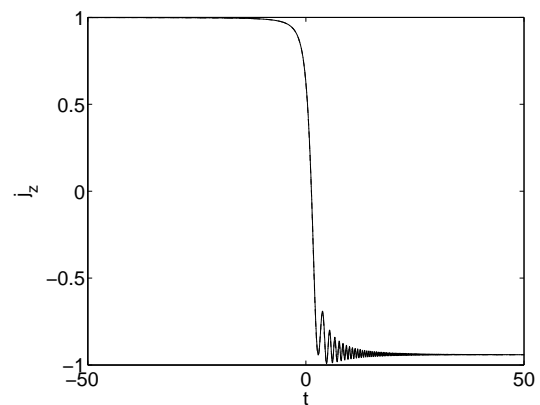


FIG. 7: The collective inversion  $j_z$  as function of time for the one dimensional case. Solid line ( $\omega = 0.01$ ), dashed line ( $\omega = 0.02$ ) and dotted line ( $\omega = 0.05$ ). The rest of the dimensionless parameters are,  $U = 1$ ,  $U_1 = 0.5$ ,  $\Delta_0 = 5$ , and  $g_{11} = g_{22} = g_{12} = 0$ .

In Fig. 7 we display examples of the collective inversion for three different trapping strengths. For these parameters the three lines are almost identical, and still for the largest  $\omega$  the ground state wave function only extends

over roughly five lattice periods. By increasing  $\omega$  further one cannot talk about a periodic system, and it is found that the momentum wave packet does not undergo a sudden momentum shift when driven through the critical point. The atom-scattering  $\mathbf{g} = 0$  in these examples.

### C. Breakdown of adiabaticity

As already pointed out, the ground state is not gapped in the current system, which should make it sensitive to non-adiabatic effects. Adiabaticity is still most likely to break down at the critical point where the density of states becomes the highest and the instantaneous energies change rapidly. In typical models, adiabaticity is expected to be violated in the thermodynamic limit  $N \rightarrow \infty$ , since then the curve crossing at the critical point becomes infinitely sharp [31]. Here, we encounter a different situation because already at the single particle level, the energies at the crossing are degenerate making it a non-avoided crossing. Thereby, the constraints for adiabaticity can be highly tested already for small atom numbers, interpreted as small scattering amplitudes  $\mathbf{g}$ .

In this section we analyze the excitations caused by non-adiabatic effects. The time evolved wave packet reads

$$\Psi(\mathbf{x}, t) = \mathcal{T} e^{-i \int_0^t \hat{H}_{GP}(t') dt'} \Psi_{GS}(\mathbf{x}), \quad (17)$$

where  $\mathcal{T}$  is the time-ordering operator and  $\Psi_{GS}(\mathbf{x})$  is given in Eq. (12). At any instant of time we can apply the imaginary time evolution to find the corresponding ground state  $\Psi_{GS}^{(t)}(\mathbf{x})$  by simply substitute  $\Psi(\mathbf{x}, t)$  into Eq. (12). We introduce the non-adiabatic relative energy increase as

$$\Delta E(t) = \frac{E_{\Psi}(t) - E_{\Psi_{GS}^{(t)}}(t)}{|E_{\Psi_{GS}^{(t)}}(t)|}, \quad (18)$$

where  $E_{\Psi}(t)$  and  $E_{\Psi_{GS}^{(t)}}(t)$  are the system energies given by the functionals  $E[\Psi]$  and  $E[\Psi_{GS}^{(t)}]$  respectively. The condition  $\partial \Delta E(t) / \partial t \ll 1$  is an indication that the evolution is adiabatic.

We note that by neglecting the spatial variation of the optical lattice,  $\cos(x) \rightarrow 1$ , the Hamiltonian (7) with the detuning (11) is identical to the Landau-Zener model [24]. A fast sweep (large  $\Delta_0$ ) implies non-adiabatic evolution and a large change in  $\Delta E(t)$ . Another possible reason for breakdown of adiabaticity is the non-linearity of the Gross-Pitaevskii equation. It is known that strong non-linearity (large values of  $\mathbf{g}$ ) tends to decrease adiabaticity [37]. On the other hand, for certain systems moderate non-linearity can even increase adiabaticity [38]. In Fig. 8 we present examples of the relative energy, both for different sweep velocities  $\Delta_0$  and different strengths  $\mathbf{g}$ . For the solid/dotted/dashed lines we use zero scattering  $\mathbf{g} = 0$ , but change the sweep velocity

$\Delta_0$ . The breakdown of adiabaticity is dominantly occurring around the critical point as expected, and moreover, fast sweeps gives a larger breakdown. The case of a non-zero scattering is depicted as a dot-dashed line in the figure. For this choice of scattering amplitudes ( $g_{11} = g_{22} = 10g_{12} = 20$ ), the adiabaticity is approximately unchanged. However, our numerical results indicates that around  $g_{11} = g_{22} = 10g_{12} = 30$  a drastic drop in the adiabaticity appears. Such sudden decrease of adiabaticity has also been demonstrated in related models [30].

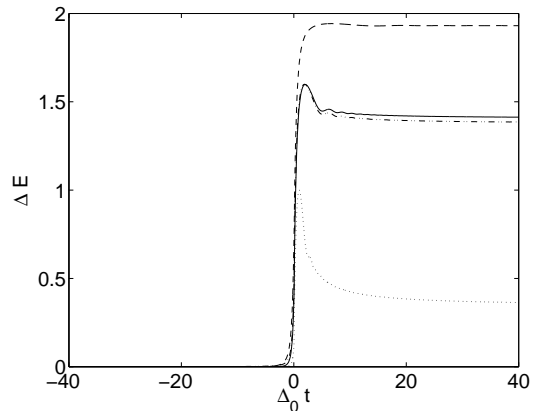


FIG. 8: The relative energy increase (18) for different sweep velocities (dotted line:  $\Delta_0 = 1$ , solid line and dot-dashed line:  $\Delta_0 = 10$ , and dashed line:  $\Delta_0 = 50$ ) and scattering amplitudes (dotted/solid/dashed lines:  $\mathbf{g} = 0$  and dot-dashed line:  $g_{11} = g_{22} = 10g_{12} = 20$ ). Increasing  $\Delta_0$  decreases the adiabaticity as predicted. The solid and dash-dotted lines correspond to the same sweep velocity but different scattering parameters  $\mathbf{g}$ , and it is noted that the non-linearity does not destroy adiabaticity in this parameter regime. However, for larger non-linearity we have found great decrease of adiabaticity. Note that we have scaled time with the sweep velocity on the  $x$ -axis. The other dimensionless parameters are as in Fig. 3 (a).

## IV. CONCLUSION

We have presented a thorough numerical analysis of spinor BEC driven through a critical point. The presence of a first order PT for the interacting system was motivated by first studying the spectrum of the single particle Hamiltonian. Since the spectrum is non-gapped, the model could be sensitive to non-adiabatic excitations. Despite this fact, it was shown by solving the full Gross-Pitaevskii equation that the PT is still clearly visible even at relatively fast sweeps through the critical point. The effects of atom-atom collisions (Fig. 4) as well as harmonic trapping (Fig. 7) were also analyzed, Both were believed to smear out signatures of the PT. However, our findings demonstrate that the PT is resilient to both. Due to limitation of computational power, most results

were carried out in the one dimensional situations, but Fig. 6 made clear that the PT is not restricted to this lower dimensional case only. As a concluding remark, the demonstrated robustness of the PT makes the current model an interesting system for experimental investigation.

## Acknowledgments

JL acknowledges support from the MEC program (FIS2005-04627).

- 
- [1] M. H. Anderson, J. R. Enscher, M. R. Matthews, C. E. Wieman, and E. A. Cornell, *Science* **269**, 198 (1995); K. B. Davies, M. O. Mewes, M. R. Andrews, N. J. VanDruten, D. S. Durfee, D. M. Kurn, and W. Ketterle, *Phys. Rev. Lett.* **75**, 3969 (1995).
- [2] C. J. Pethick and H. Smith, *Bose-Einstein Condensation in Dilute Gases*, (Cambridge University Press, Cambridge 2008).
- [3] C. J. Myatt, E. A. Burt, R. W. Ghrist, E. A. Cornell, and C. E. Wieman, *Phys. Rev. Lett.* **78**, 586 (1997); J. Stenger, S. Inouye, D. M. Stamper-Kurn, H.-J. Miesner, A. P. Chikkatur, and W. Ketterle, *Nature* **396**, 345 (1998); M. S. Chang, C. D. Hamley, M. D. Barrett, J. A. Sauer, K. M. Fortier, W. Zhang, L. You, and M. S. Chapman, *Phys. Rev. Lett.* **92**, 140403 (2004).
- [4] O. Mandel, M. Greiner, A. Widera, T. Rom, T. W. Hänsch, and I. Bloch, *Phys. Rev. Lett.* **91**, 010407 (2003).
- [5] M. S. Chang, C. D. Hamley, M. D. Barrett, J. A. Sauer, K. M. Fortier, W. Zhang, L. You, and M. S. Chapman, *Phys. Rev. Lett.* **92**, 140403 (2004).
- [6] D. M. Stamper-Kurn, H. J. Miesner, A. P. Chikkatur, S. Inouye, J. Stenger, and W. Ketterle, *Phys. Rev. Lett.* **83**, 661 (1999).
- [7] L. E. Sadler, J. M. Higbie, S. R. Leslie, M. Vengalattore, and M. S. Stamper-Kurn, *Nature* **443**, 312 (2006).
- [8] O. Morsch, J. H. Müller, M. Cristiani, D. Ciampini, and E. Arimondo, *Phys. Rev. Lett.* **87**, 140402 (2001).
- [9] B. Eiermann, T. Anker, M. Albiez, M. Taglieber, P. Treutlein, K. P. Marzlin, M. K. Oberthaler, *Phys. Rev. Lett.* **92**, 230401 (2004).
- [10] Z. D. Li, P. B. He, J. Q. Liang, and W. M. Liu, *Phys. Rev. A* **71**, 053611 (2004).
- [11] B. B. Wang, P. M. Fu, J. Liu, and B. Wu, *Phys. Rev. A* **74**, 063610 (2006).
- [12] J. Mun, P. Medley, G. K. Campbell, L. G. Marcassa, D. E. Pritchard, and W. Ketterle, arXiv:0706.3946.
- [13] J. W. Reijnders and R. A. Duine, *Phys. Rev. Lett.* **93**, 060401 (2004).
- [14] B. Juliette, V. Josse, Z. Zuo, A. Bernard, B. Hembrecht, P. Lugan, D. Clément, L. Sanchez-Palencia, P. Bouyer, and A. Aspect, *Nature* **453**, 891 (2008).
- [15] M. Greiner, O. Mandel, T. Esslinger, T. W. Hänsch, and I. Bloch, *Nature* **415**, 39 (2002).
- [16] M. Lewenstein, A. Sanpera, V. Ahufinger, B. Damski, A. Sen, and U. Sen, *Adv. Phys.* **56**, 243 (2007); I. Bloch, J. Dalibard, and W. Zwerger, *Rev. Mod. Phys.* **80**, 885 (2008).
- [17] W. H. Zurek, U. Dorner, and P. Zoller, *Phys. Rev. Lett.* **95**, 105701 (2005).
- [18] J. Dziarmaga, *Phys. Rev. Lett.* **95**, 245701 (2005); T. Caneva, R. Fazio, and G. E. Santoro, *Phys. Rev. B* **76**, 144427 (2007); V. Mukherjee, U. Divakaran, A. Dutta, and D. Sen, *Phys. Rev. B* **76**, 174303 (2007); F. Pellegrini, S. Montangero, G. E. Santoro, and R. Fazio, *Phys. Rev. B* **77**, 140404(R) (2008).
- [19] T. Caneva, R. Fazio, and G. E. Santoro, *Phys. Rev. B* **78**, 104426 (2008); P. Solinas, P. Riberio, and R. Mosseri, *Phys. Rev. A* **78**, 052329 (2008).
- [20] K. Sengupta, D. Sen, and S. Mondal, *Phys. Rev. Lett.* **100**, 077204 (2008); S. Mondal, D. Sen, and K. Sengupta, *Phys. Rev. B* **78**, 045101 (2008).
- [21] H. T. Quan, Z. D. Wang, and C. P. Sun, *Phys. Rev. A* **76**, 012104 (2007).
- [22] A. Polkovnikov, *Phys. Rev. B* **72**, 161201(R) (2005); F. M. Cucchiatti, B. Damski, J. Dziarmaga, and W. H. Zurek, *Phys. Rev. A* **75**, 023603 (2007).
- [23] J. Dziarmaga, J. Meisner, and W. H. Zurek, *Phys. Rev. Lett.* **101**, 115701 (2008).
- [24] L. D. Landau, *Phys. Z. Sowjet Union* **2**, (1932); C. Zener, *Proc. Roy. Soc. Lond. A* **137**, 696 (1932).
- [25] J. Larson and J.-P. Martikainen, *Phys. Rev. A* **78**, 063618 (2008).
- [26] J. Larson and J.-P. Martikainen, arXiv:0811.4147.
- [27] M. Alexanian and S. K. Bose, *Phys. Rev. A* **52**, 2218 (1995).
- [28] W. Ren and H. J. Carmichael, *Phys. Rev. A* **51**, 752 (1995); J. Larson, J. Salo, and S. Stenholm, *Phys. Rev. A* **72**, 013814 (2005).
- [29] K. V. Krutitsky and R. Graham, *Phys. Rev. Lett.* **91**, 240406 (2003); *ibid.*, *Phys. Rev. A* **70**, 063610 (2004).
- [30] B. Wu, R. B. Diener, and Q. Niu, *Phys. Rev. A* **65**, 025601 (2002); M. Machholm, C. J. Pethick, and H. Smith, *Phys. Rev. A* **67**, 053613 (2003).
- [31] S. Sachdev, *Quantum Phase Transition*, (Cambridge University Press, Cambridge 1998).
- [32] M. D. Fleit, J. A. Fleck, and A. Steiger, *J. Comp. Phys.* **47**, 412 (1982).
- [33] W. L. You, Y. W. Li, and S.-J. Gu, *Phys. Rev. E* **76**, 022101 (2007).
- [34] S.-J. Gu, H.-M. Kwok, W.-Q. Ning, and H.-Q. Lin, *Phys. Rev. B* **77**, 245109 (2008).
- [35] S. Yang, S.-J. Gu, C.-P. Sun, and H.-Q. Lin, *Phys. Rev. A* **78**, 012304 (2008).
- [36] H.-M. Kwok, C.-S. Ho, and S.-J. Gu, *Phys. Rev. A* **78**, 062302 (2008).
- [37] B. Wu and Q. Niu, *Phys. Rev. A* **61**, 023402 (2000).
- [38] A. P. Itin and S. Watanabe, *Phys. Rev. Lett.* **99**, 223903 (2007).